

## Structure and photoluminescence of $(\text{Ca,Eu})_2\text{SiS}_4$ powders

This article has been downloaded from IOPscience. Please scroll down to see the full text article.

2007 J. Phys.: Condens. Matter 19 246223

(<http://iopscience.iop.org/0953-8984/19/24/246223>)

View [the table of contents for this issue](#), or go to the [journal homepage](#) for more

Download details:

IP Address: 129.252.86.83

The article was downloaded on 28/05/2010 at 19:15

Please note that [terms and conditions apply](#).

# Structure and photoluminescence of $(\text{Ca}, \text{Eu})_2\text{SiS}_4$ powders

P F Smet<sup>1</sup>, N Avci, B Loos, J E Van Haecke and D Poelman

LumiLab, Department of Solid State Sciences, Ghent University (UGent), Krijgslaan 281-S1, 9000 Gent, Belgium

E-mail: [philippe.smet@ugent.be](mailto:philippe.smet@ugent.be)

Received 8 March 2007, in final form 10 May 2007

Published 30 May 2007

Online at [stacks.iop.org/JPhysCM/19/246223](http://stacks.iop.org/JPhysCM/19/246223)

## Abstract

The photoluminescence of  $\text{Ca}_2\text{SiS}_4:\text{Eu}$  powders was investigated in detail as a function of europium concentration (from 0.1% Ca substitution to the fully substituted  $\text{Eu}_2\text{SiS}_4$ ). At low europium dopant concentration (<10%) the powders crystallize in an orthorhombic structure and the emission spectrum is dominated by two broad emission bands, at 564 and 660 nm. The emission can be tuned from yellow (CIE  $x = 0.46$ ,  $y = 0.53$ ) to red (CIE  $x = 0.65$ ,  $y = 0.35$ ) by variation of the Eu concentration. An energetic coupling exists between both bands, leading to a broad excitation wavelength range. Powders with high europium concentration (>40%) crystallize in a monoclinic structure, details of which were determined by Rietveld refinement of x-ray diffraction data. For the composition  $\text{CaEuSiS}_4$  (i.e. 50% substitution), the luminescence peaks at 614 nm, shifting to shorter wavelengths upon further substitution of Ca by Eu. Although considerable thermal quenching is present at room temperature in the fully Eu-substituted compound,  $\text{Eu}_2\text{SiS}_4$  is still photoluminescent, with a peak emission wavelength of 577 nm. A strong correlation is found between the crystallographic and luminescent properties of the  $(\text{Ca}, \text{Eu})_2\text{SiS}_4$  powders. The broad emission and excitation bands make this phosphor a good candidate for use in phosphor-converted light-emitting diodes (pcLEDs).

## 1. Introduction

Research in the field of luminescent materials has been continuous and intensive over the past century. Every time new technologies emerged, phosphor materials fulfilling specific requirements were investigated and developed. For instance, CRTs (cathode ray tubes) required good cathodoluminescent phosphors, while the emergence of FEDs (field emission displays) initiated a search for efficient phosphors working at low electron energies. The development of other technologies, such as plasma displays, inorganic thin film electroluminescence and

<sup>1</sup> Author to whom any correspondence should be addressed.

phosphor-converted LEDs for solid-state lighting, also showed the need for ‘new’ materials with specific properties. Given the fact that an inorganic luminescent material mostly consists of a host material with a relatively small but controlled amount of impurities (the dopants), the possible number of phosphor materials is very high. For instance, Dorenbos recently listed more than 300  $\text{Eu}^{2+}$ -doped luminescent compounds [1].

More particularly in the field of thin film electroluminescence, research has shifted in the past decade from binary sulfide hosts towards rare-earth doped ternary sulfides, such as  $\text{SrGa}_2\text{S}_4:\text{Ce}$  and  $\text{BaAl}_2\text{S}_4:\text{Eu}$  [2–4]. Although certain transition metals (such as Cu, Ag [5] and Pb [6]) were proposed as dopant ions as well, the broad-band emitting rare-earth ions  $\text{Ce}^{3+}$  and  $\text{Eu}^{2+}$  are currently being studied intensively. The emission in these ions originates from 5d–4f transitions, for which the emission energy depends strongly on the crystal field strength. Hence the emission colour can be tuned over the entire visible part of the spectrum by variation of the host material. Given the relatively small number of suitable binary hosts, ternary and even quaternary hosts are used to arrive at the desired emission properties. Currently,  $\text{Ba}_{1-x}\text{Mg}_x\text{Al}_2\text{S}_4:\text{Eu}$  appears to be a good candidate for the blue emission in inorganic thin-film electroluminescent (EL) displays, although the limited stability of the phosphor upon contact with moisture is still a major issue [7]. Consequently, the search towards new materials continues.

Recently, photoluminescent sulfides have also come into the picture for use in phosphor-converted light-emitting diodes (pcLEDs), as these solid-state devices are very attractive for general lighting purposes [8–11]. In these devices, the emitted light of a near-ultraviolet (or blue) LED is (partly) down-converted by a phosphor to arrive at the desired emission spectrum. If necessary, a combination of phosphors is used to obtain good colour rendering in the case of white-emitting LEDs. Although many photoluminescent powders have been developed and optimized for fluorescent tubes, the requirements for LEDs are different, as a much smaller Stokes’ shift is needed for pcLEDs. Currently, yellow-emitting YAG:Ce is often used in pcLEDs, although this phosphor material lacks sufficient emission in the red. (Ca, Sr)S:Eu has been proposed as an orange-red emitting phosphor [12]. Mueller-Mach *et al* recently reported on  $\text{Eu}^{2+}$ -doped nitrides [9].

In this work we focus on the properties of europium-doped calcium thiosilicate ( $\text{Ca}_2\text{SiS}_4:\text{Eu}$ ). Although the rare-earth doped thiosilicate phosphors were first investigated in the 1970s, these materials have attracted surprisingly little attention since then [13, 14]. Beside structural characterization of  $\text{Ca}_2\text{SiS}_4$  (space group  $P_{nma}$ , orthorhombic [15]) and  $\text{Eu}_2\text{SiS}_4$  (space group  $P2_1/m$ , monoclinic [16]), the luminescent properties of  $\text{Ca}_2\text{SiS}_4:\text{Eu}$  have been explored only briefly. Avella reported that the cathodoluminescence is characterized by an emission peak at 563 nm [14]. A second emission band peaking at 660 nm was also observed, and tentatively assigned to the presence of CaS:Eu in the synthesized powder. Avella also reported that the cathodoluminescent emission was very weak compared to that of  $\text{Sr}_2\text{SiS}_4:\text{Eu}$  and  $\text{Ba}_2\text{SiS}_4:\text{Eu}$  [14]. Recently, Samura *et al* prepared Ce-doped  $\text{Ba}_2\text{SiS}_4$  and  $\text{Sr}_2\text{SiS}_4$  thin films by electron-beam evaporation [17].

Here we report in detail on the structural and photoluminescent properties of (Ca, Eu) $_2\text{SiS}_4$  powders. We show that this material should be reconsidered, given the excellent photoluminescent properties (at least for certain compositions). Finally, we evaluate the possible application in pcLEDs.

## 2. Experimental setup

$\text{Ca}_2\text{SiS}_4:\text{Eu}$  powders were prepared by sintering a mixture of CaS (Cerac, 99.99%) and Si (Alfa Aesar, 99.5%) powders in a continuous flow of  $\text{H}_2\text{S}$  at 950 °C (during 1 h). Compared to many

**Table 1.** Crystallographic data obtained by Rietveld refinement of the x-ray diffraction patterns of  $(\text{Ca, Eu})_2\text{SiS}_4$  powders with various composition. The errors on the last digit in the refined crystallographic parameters are given between brackets.

	Space group	$a$ (pm)	$b$ (pm)	$c$ (pm)	$\beta$ (deg)	Reference
$\text{Ca}_2\text{SiS}_4$	$Pnma$	1349	818	621		[15]
$\text{Ca}_2\text{SiS}_4$	$Pnma$	1352 (2)	819 (1)	621 (1)		This work
$\text{Ca}_{1.8}\text{Eu}_{0.2}\text{SiS}_4$	$Pnma$	1353 (2)	822 (1)	621 (1)		This work
$\text{Ca}_{1.2}\text{Eu}_{0.8}\text{SiS}_4$	$P2_1/m$	648 (1)	660 (1)	793 (1)	107.9 (1)	This work
$\text{CaEuSiS}_4$	$P2_1/m$	650 (1)	660 (1)	799 (1)	108.1 (1)	This work
$\text{Ca}_{0.75}\text{Eu}_{1.25}\text{SiS}_4$	$P2_1/m$	650 (1)	660 (1)	801 (1)	108.0 (1)	This work
$\text{Ca}_{0.5}\text{Eu}_{1.5}\text{SiS}_4$	$P2_1/m$	651 (1)	659 (1)	807 (1)	108.2 (1)	This work
$\text{Ca}_{0.2}\text{Eu}_{1.8}\text{SiS}_4$	$P2_1/m$	651 (1)	660 (1)	815 (1)	108.3 (1)	This work
$\text{Ca}_{0.1}\text{Eu}_{1.9}\text{SiS}_4$	$P2_1/m$	651 (1)	659 (1)	817 (1)	108.4 (1)	This work
$\text{Eu}_2\text{SiS}_4$	$P2_1/m$	651 (1)	660 (1)	820 (1)	108.4 (1)	This work
$\text{Eu}_2\text{SiS}_4$	$P2_1/m$	652	660	822	108.4	[16]

other ternary sulfide compounds, this is a rather low synthesis temperature. Eu doping was obtained by using  $\text{EuF}_3$  (Cerac, 99.9%) for the powders with low europium concentration (up to 2%), while  $\text{EuS}$  was used for higher concentrations. The  $\text{EuS}$  was prepared by sulfurizing high-purity  $\text{Eu}_2\text{O}_3$  in a stream of  $\text{H}_2\text{S}$  at  $900^\circ\text{C}$  [18]. Si was used instead of  $\text{SiS}_2$ , as  $\text{SiS}_2$  quickly degrades upon contact with ambient air. Furthermore, high-purity  $\text{SiS}_2$  is not commercially available. The sulfur required to obtain stoichiometric  $\text{Ca}_2\text{SiS}_4\cdot\text{Eu}$  was provided by the  $\text{H}_2\text{S}$  atmosphere. It was observed that powders were of lower quality if, instead, sulfur powder was added to the initial mixture. Dopant concentrations mentioned in this work are molar concentrations, i.e. the percentage of Ca substituted by Eu.

X-ray diffraction patterns were recorded using a Bruker D5000 diffractometer, in standard  $\theta$ - $2\theta$  geometry using  $\text{Cu K}\alpha$  radiation. Structural information, such as values for the lattice constants, was obtained using the Rietveld refinement method with the Fullprof software package [19]. The Rietveld refinement was used to determine the lattice constants of the  $(\text{Ca, Eu})_2\text{SiS}_4$  compounds, based on structural information for  $\text{Ca}_2\text{GeS}_4$  and  $\text{Eu}_2\text{SiS}_4$ . Neither the atomic positions in the unit cell nor the atomic displacement parameters were refined. The goodness of fit was evaluated graphically [20]. Silicon powder was added as an internal standard for improving accuracy. Photoluminescence emission and excitation spectra were recorded using a FS920 fluorescence spectrometer (Edinburgh Instruments). Decay constants were obtained using a setup with a pulsed nitrogen laser ( $\lambda_{\text{exc}} = 337$  nm, pulse length 800 ps, repetition rate 1 Hz) and a 1024-channel intensified CCD attached to a 0.5 m Ebert monochromator.

### 3. Results

#### 3.1. Structural characterization

**3.1.1. Undoped  $\text{Ca}_2\text{SiS}_4$  and low Eu substitution.** Before discussing the influence of europium substitution, we consider the crystallographic structure of undoped  $\text{Ca}_2\text{SiS}_4$ . The lattice constants are in correspondence with earlier reports (table 1), regardless of the fact that the preparation technique used in this work (i.e. sintering an intimate mixture of  $\text{CaS}$  and  $\text{Si}$  in  $\text{H}_2\text{S}$ ) differs from previous reports [14].

We checked the effect of adding elemental sulfur to the starting mixture. However, this resulted in powders with a much darker body colour (pointing at a higher defect concentration)

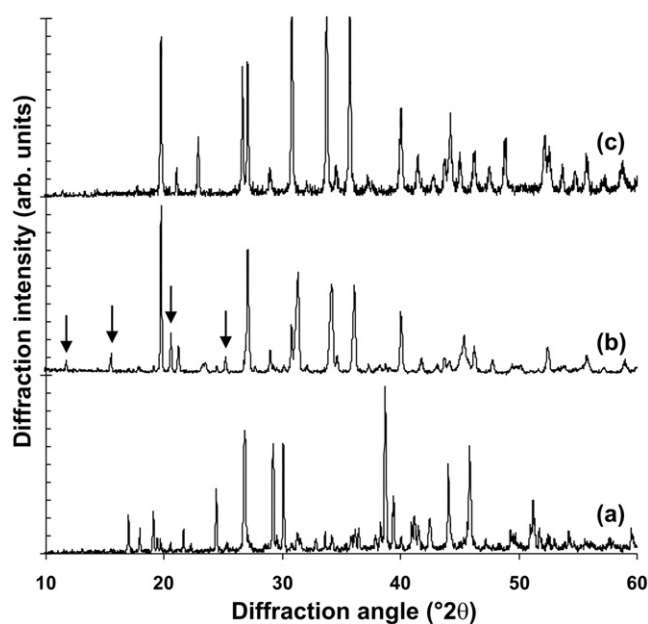


**Figure 1.** X-ray diffraction pattern for (a)  $\text{Ca}_{1.8}\text{Eu}_{0.2}\text{SiS}_4$ , (b)  $\text{CaEuSiS}_4$  and (c)  $\text{Eu}_2\text{SiS}_4$  powders. For the meaning of the arrows in (b), see text.

and poor stability upon contact with ambient air. Based on x-ray diffraction measurements, we observed that, upon preparing the starting mixture with the stoichiometric molar ratio (CaS:Si equal to 2:1), trace amounts of CaS were present after the sintering process. This was not due to an incomplete or inhomogeneous solid-state reaction, as regrinding and a second sintering did not eliminate these diffraction peaks. Submicron  $\text{SiO}_2$  particles (not observed in x-ray diffraction) could be detected using scanning electron microscopy combined with energy-dispersive x-ray (EDX) elemental analysis. It is also possible that part of the Si is lost by the formation of volatile compounds, as the synthesis was performed in an open crucible [21]. Increasing the CaS:Si ratio to 2.00:1.05 led to a single-phase powder (i.e.  $\text{Ca}_2\text{SiS}_4$ ), without the presence of CaS. For the remaining part of this work, this Ca + Eu:Si molar ratio of 2.00:1.05 was used.

As the ionic radius of  $\text{Eu}^{2+}$  is larger than that of  $\text{Ca}^{2+}$ , it can be expected that substitution of  $\text{Ca}^{2+}$  ions in  $\text{Ca}_2\text{SiS}_4$  by  $\text{Eu}^{2+}$  leads to an increase in the lattice constants. In the (identical) crystal structure of CaS and EuS, the Ca–S distance is 285 pm, while this distance is 298 pm for EuS. For 10% substitution (i.e.  $\text{Ca}_{1.8}\text{Eu}_{0.2}\text{SiS}_4$ , figure 1(a)), the unit cell indeed slightly expands compared to  $\text{Ca}_2\text{SiS}_4$  (table 1). Upon a further increase in the europium concentration, a second crystallographic phase, isostructural with  $\text{Eu}_2\text{SiS}_4$ , starts to appear.

**3.1.2.  $(\text{Ca}, \text{Eu})_2\text{SiS}_4$  with high Eu concentration.**  $\text{Eu}_2\text{SiS}_4$  was reported to be monoclinic with space group  $P2_1/m$  [16, 22]. This structure determination was performed on single crystals, prepared out of molar amounts of Eu, S and  $\text{SiS}_2$  in evacuated silica tubes. In our work, the prepared  $\text{Eu}_2\text{SiS}_4$  powders show the same structure, and the derived lattice constants correspond to the literature data (table 1, figure 1(c)). Given the different crystallographic structures for the pure compounds  $\text{Ca}_2\text{SiS}_4$  and  $\text{Eu}_2\text{SiS}_4$ , it is interesting to study the phase formation in  $(\text{Ca}, \text{Eu})_2\text{SiS}_4$  powders as a function of the Ca:Eu ratio. Only the monoclinic

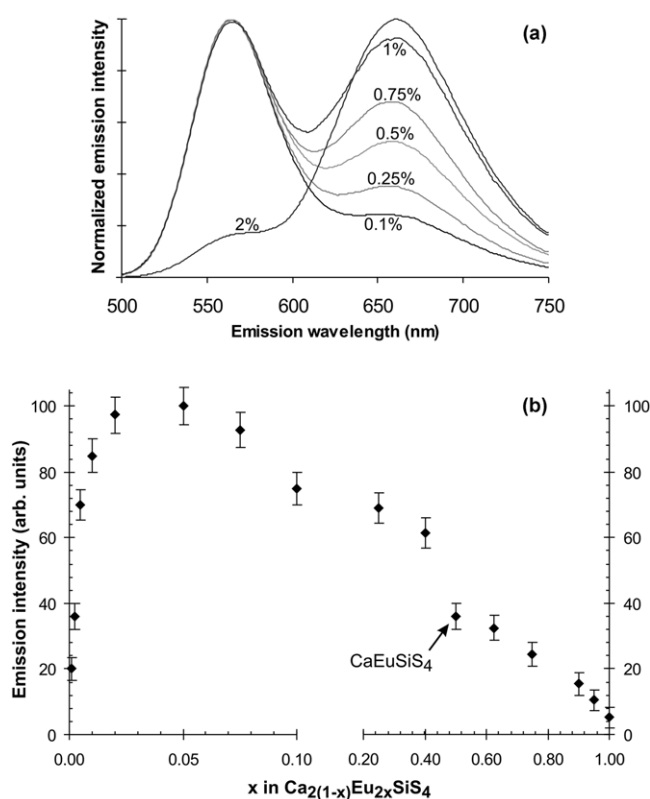


**Figure 2.** (a) Normalized photoluminescence emission spectra of  $(\text{Ca}, \text{Eu})_2\text{SiS}_4$  powders as a function of the europium concentration. Spectra were recorded at room temperature and with an excitation wavelength of 400 nm. (b) Photoluminescence emission intensity upon excitation at 400 nm for  $\text{Ca}_{2(1-x)}\text{Eu}_{2x}\text{SiS}_4$  powders.

structure is obtained for the powders in the range from  $\text{Ca}_{0.8}\text{Eu}_{1.2}\text{SiS}_4$  to  $\text{Eu}_2\text{SiS}_4$ . Substitution of Eu by Ca leads to a reduced unit cell volume due to the smaller ionic radius of Ca compared to Eu. However, the shrinkage of the unit cell is not isotropic. Table 1 shows the values of the unit cell parameters for several compounds from  $\text{Ca}_{0.8}\text{Eu}_{1.2}\text{SiS}_4$  to  $\text{Eu}_2\text{SiS}_4$ . While the value of  $b$  remains roughly unchanged and  $a$  reduces slightly for higher Ca concentration,  $c$  strongly decreases upon substitution of Eu by Ca. Furthermore, for increasing Ca concentrations, the intensity of several diffraction peaks increases compared to  $\text{Eu}_2\text{SiS}_4$  (some of these peaks at low diffraction angle are indicated by arrows in figure 1(b)). Using the Rietveld refinement method [19], this could be related to a preferential substitution of Eu by Ca on the Eu2 position, as defined by Hartenbach *et al* [16]

**3.1.3. Intermediate compositions.** Synthesis of  $(\text{Ca}, \text{Eu})_2\text{SiS}_4$  powders with a Ca concentration in the range from 15 to 40% does not result in a single-phase material, as the orthorhombic  $\text{Ca}_2\text{SiS}_4$ -like and the monoclinic  $\text{Eu}_2\text{SiS}_4$ -like phases coexist. Given this relatively broad overlap range, we can conclude that there is no sharp phase transition between both phases as a function of the Ca:Eu ratio.

### 3.2. Photoluminescent characterization

**3.2.1. Low Eu concentration.** Figure 2 shows the photoluminescence spectra of  $\text{Ca}_2\text{SiS}_4:\text{Eu}$  powders as a function of europium concentration. At low concentration (0.1%), the emission spectrum is dominated by an emission band at 564 nm (full width at half maximum, FWHM:

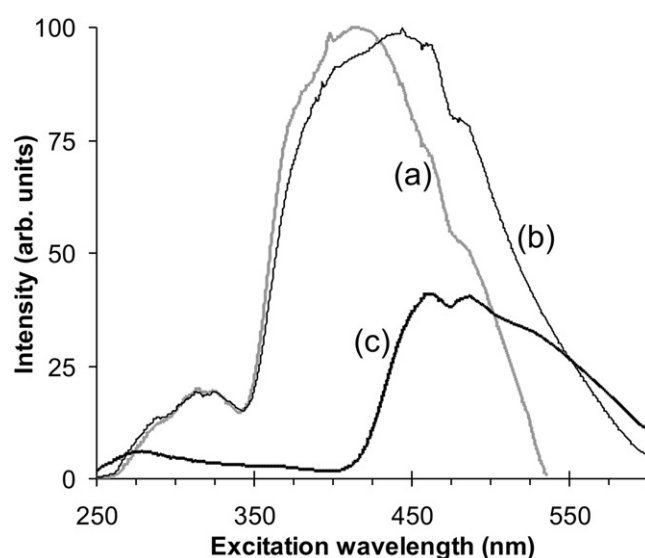


**Figure 3.** Excitation spectra for  $\text{Ca}_2\text{SiS}_4:\text{Eu}$  and  $\text{CaS}:\text{Eu}$  measured at room temperature. (a) The yellow emission in  $\text{Ca}_2\text{SiS}_4:\text{Eu}$  [0.5%], monitored at 560 nm, (b)  $\text{Ca}_2\text{SiS}_4:\text{Eu}$  [0.5%], monitored at 660 nm, (c)  $\text{CaS}:\text{Eu}$  [0.1%], monitored at 660 nm.

60 nm), originating from  $4f^65d$  to  $4f^7$  transitions in  $\text{Eu}^{2+}$ . A second, much weaker emission band at longer wavelengths is also visible. The origin of this emission band will be discussed below. This leads to CIE coordinates of (0.46, 0.53), corresponding to yellow emission.

Upon an increase of the europium concentration, the second emission band, centred at 660 nm, now clearly emerges, and dominates the emission spectrum for a concentration higher than 1% (figure 2(a)). For a europium concentration of 5%, CIE coordinates of (0.65, 0.35) are obtained, which corresponds to a saturated red emission [23]. The emission spectra are in line with the work on  $\text{Ca}_2\text{SiS}_4:\text{Eu}$  by Avella, who used a dopant concentration of 0.25 or 0.5%. He reported a peak emission wavelength of 563 nm and a FWHM of 63 nm, along with a second emission band at 660 nm [14].

Preliminary measurements indicate that the external quantum efficiency upon excitation at 462 nm is 35% for  $\text{Ca}_2\text{SiS}_4:\text{Eu}$  [2%], which is in strong contrast to the reported poor efficiency in cathodoluminescence [14]. After fine tuning the sintering conditions, this value might still be improved.

The influence of temperature (studied in the range from 70 to 320 K) on the spectrum and the intensity of the  $(\text{Ca}, \text{Eu})_2\text{SiS}_4$  emission was studied on a selected number of compositions. Lowering the temperature leads to a narrowing of the two emission bands due to the occupation of lower vibrational levels. However, the relative intensity of the two peaks (and also their position) is almost independent on temperature, which leads to a stable emission colour.

Figure 3 shows the excitation spectra for both emission peaks, monitored at 560 and at 660 nm. The form of these spectra is characteristic for  $4f^7-4f^65d$  transitions in  $\text{Eu}^{2+}$ . Depending on the exact site symmetry, the 5d levels splits in multiple components, and at least two bands are observed. No fine structure due to the  $^7F_J$  levels in the  $4f^6$  configuration can be discerned [24]. The interpretation of the excitation spectra is further complicated by the presence of two emission centres and by possible overlap with band gap transitions of the host  $\text{Ca}_2\text{SiS}_4$  crystal. More research is required to elucidate all the details of the excitation spectrum. It is striking, however, that the excitation bands coincide for both emission centres



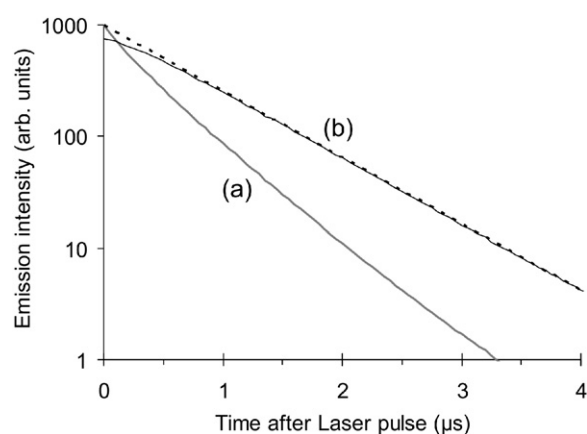


**Figure 4.** Decay profiles for (a) the yellow emission and (b) the red emission in  $\text{Ca}_2\text{SiS}_4:\text{Eu}$  [0.75%] upon pulsed excitation (pulse length  $< 1$  ns). For the red emission, a single exponential decay profile is shown with a dotted line.

on the high-energy side. This points to the fact that the red emission band is efficiently excited *via* the yellow emission centre. Consequently, the excitation spectrum for the red emission band ranges from 350 to 550 nm. This is much wider than that from  $\text{CaS}:\text{Eu}$  powder, which is shown for comparison in figure 3. For pcLED application, the excitation bands should have a large overlap with the emission of near-UV and blue LEDs, which is indeed the case.

From the excitation spectra, it is clear that some kind of energy transfer occurs between both emission bands in  $\text{Ca}_2\text{SiS}_4:\text{Eu}$ . To prove this concept, luminescent decay spectra were recorded using a pulsed nitrogen laser with an excitation wavelength of 337.1 nm. Figure 4 shows the decay profile for the yellow and the red emission bands. The yellow emission band shows a slightly faster than exponential decay for a europium concentration of 0.1%, with a main decay constant of 550 ns. The red emission band is characterized by a single decay constant of 710 ns, apart from the initial part of the decay, where the decay is subexponential. This can be explained by ‘pumping’ of the red emission, *via* the yellow emitting centres. Increasing the dopant concentration has no effect on the main decay constant of the red emission, however the yellow emission decays faster, as two components are clearly observed in the decay profile (table 2). The relative intensity of the fast decay component increases with increasing dopant concentration, indicating an increased transfer to the red emission band. The main decay constant of the red emission is hardly affected by a large dopant concentration, even for 10% Eu ( $\tau = 0.68 \mu\text{s}$ ). At high dopant concentration an additional, a faster decay component is however observed in the decay profiles. This can be related to the saturation of the emission intensity upon an increase in the europium concentration beyond 2% (figure 2(b)), pointing to the increased presence of non-radiative decay routes. Nevertheless, as shown in figure 2(b), the photoluminescence is still efficient for higher dopant concentrations.

The emission colour of the powders (determined by the relative intensity of both emission bands) was also studied as a function of the power of the incident excitation light. Using a 200 mW Ar laser (corresponding to a maximum excitation intensity of about  $30 \text{ W cm}^{-2}$ ), no appreciable differences in the emission colour were observed as a function of the incident power. Only by using a pulsed nitrogen laser (peak power density of about  $10 \text{ W cm}^{-2}$ ) could we observe a relative reduction in the red emission band at high power (not shown), which is in line with a saturation of the energy transfer from the yellow to the red emission centre. However, the effect is marginal in practical situations, even for the power densities typical for



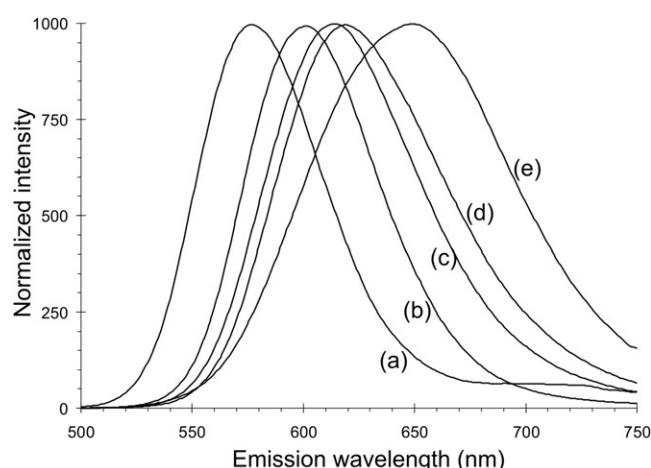


**Figure 5.** Emission spectra of  $(\text{Ca}, \text{Eu})_2\text{SiS}_4$  powders measured at an excitation wavelength of 400 nm: (a)  $\text{Eu}_2\text{SiS}_4$ , (b)  $\text{Ca}_{0.5}\text{Eu}_{1.5}\text{SiS}_4$ , (c)  $\text{CaEuSiS}_4$ , (d)  $\text{Ca}_{1.2}\text{Eu}_{0.8}\text{SiS}_4$ ; (e) is the emission spectrum for the powder with intended composition  $\text{Ca}_{1.5}\text{Eu}_{0.5}\text{SiS}_4$ . See text for more details.

**Table 2.** Influence of the europium concentration on the colour coordinates of  $(\text{Ca}, \text{Eu})_2\text{SiS}_4$  powders. Coordinates were calculated based on emission spectra recorded at an excitation wavelength of 400 nm. Decay constants are given for the yellow and the red emission band. If two components are found, then the data between brackets refer to the total emitted intensity assigned to this component. All data were obtained at room temperature.

Eu conc.(molar %)	CIE 1931 colour coordinates		Decay constants ( $\mu\text{s}$ , $\pm 0.01 \mu\text{s}$ )		
	CIE x	CIE y	Yellow		Red
0.10	0.46	0.53	0.21 (9%)	0.55 (91%)	0.72
0.25	0.47	0.52	0.22 (20%)	0.54 (80%)	0.72
0.50	0.48	0.51	0.22 (24%)	0.52 (76%)	0.72
0.75	0.49	0.50	0.22 (33%)	0.50 (67%)	0.72
1.0	0.52	0.48	0.22 (51%)	0.49 (49%)	0.71
2.0	0.57	0.42	0.21 (58%)	0.47 (42%)	0.69
5.0	0.65	0.35	0.13	—	0.69
7.5	0.66	0.34	0.10	—	0.68
10.0	0.66	0.34	—	—	0.68

high-brightness pcLEDs. Hence, application of the  $(\text{Ca}, \text{Eu})_2\text{SiS}_4$  phosphors in LEDs leads to a stable emission colour.

**3.2.2. High Eu concentration.** Figure 5 shows the luminescence spectrum of the  $(\text{Ca}, \text{Eu})_2\text{SiS}_4$  powders with high europium content, ranging from  $\text{Ca}_{1.2}\text{Eu}_{0.8}\text{SiS}_4$  to  $\text{Eu}_2\text{SiS}_4$ . In section 3.1.2 it was already shown that all these powders crystallize in the monoclinic,  $\text{Eu}_2\text{SiS}_4$ -like crystallographic structure. In the range from  $\text{CaEuSiS}_4$  to  $\text{Eu}_2\text{SiS}_4$ , the peak of the emission band shifts almost linearly with composition from 614 to 577 nm, respectively.

From the decay profiles in figure 6, one readily sees that the luminescent decay proceeds faster as the europium concentration increases, with deviations from a single exponential decay. For instance,  $\text{Eu}_2\text{SiS}_4$  has a main decay constant of about 45 ns at room temperature, while this increases to 250 ns at 70 K (not shown). It is clear that non-radiative decay paths become

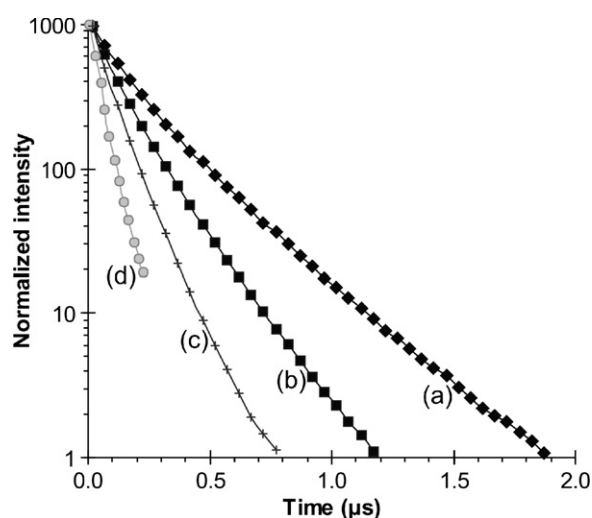


**Figure 6.** Decay profiles of the luminescence emission intensity upon excitation at 337 nm, measured at room temperature for (a)  $\text{CaEuSi}_4$ , (b)  $\text{Ca}_{0.5}\text{Eu}_{1.5}\text{Si}_4$ , (c)  $\text{Ca}_{0.2}\text{Eu}_{1.8}\text{Si}_4$ , (d)  $\text{Eu}_2\text{Si}_4$ .

increasingly important upon an increase in europium concentration, as the distance between the dopant ions decreases accordingly. Furthermore, the compounds with high europium concentration suffer from considerable thermal quenching, which is also related to the presence of these non-radiative decay routes. Hence the photoluminescence efficiency of the powders with high dopant concentration ( $>50\%$ ) is relatively low (figure 2(b)).

**3.2.3. Intermediate compositions.** Based on the x-ray diffraction patterns of  $(\text{Ca}, \text{Eu})_2\text{Si}_4$  powders discussed in section 3.1.3, we observed no sharp transition between the orthorhombic and the monoclinic phase as a function of the composition. For an Eu concentration between 15 and 40%, both phases coexist, which is also reflected in the emission spectrum of these powders. Figure 7 shows the emission spectrum for the powder with an intended composition of  $\text{Ca}_{1.5}\text{Eu}_{0.5}\text{Si}_4$ . The emission band is rather broad (FWHM: 108 nm) and asymmetric. The emission spectrum can be fitted very well by contributions from the (single phase) compounds  $\text{Ca}_{1.8}\text{Eu}_{0.2}\text{Si}_4$  and  $\text{Ca}_{1.2}\text{Eu}_{0.8}\text{Si}_4$  (figure 7).

#### 4. Discussion

As shown above, the crystallographic structure of the  $(\text{Ca}, \text{Eu})_2\text{Si}_4$  powders is reflected in the photoluminescence emission spectra. The emission of  $\text{Eu}_2\text{Si}_4$  is characterized by a single emission band at 577 nm, while  $\text{CaEuSi}_4$  shows a single emission band at 614 nm. For the intermediate concentrations, the luminescence shifts monotonically with composition. Simultaneously, the lattice shows an anisotropic contraction along the  $c$ -axis from  $\text{Eu}_2\text{Si}_4$  to  $\text{CaEuSi}_4$ . In general, shorter Eu–S bonding distances lead to a lower emission energy of the Eu 5d–4f transition due to an increase in the crystal field strength. For instance, the peak emission wavelength shifts from 620 nm in  $\text{SrS:Eu}$  to 652 nm in  $\text{CaS:Eu}$  for a corresponding 5% decrease in the Eu–S bond length. Based on the structure refinement of  $\text{Eu}_2\text{Si}_4$  [16], it is not surprising that the lattice shrinks anisotropically along the  $c$ -axis upon Ca substitution, as the Eu atoms occupy positions on chains parallel to the  $c$ -axis, with an Eu–Eu distance of on

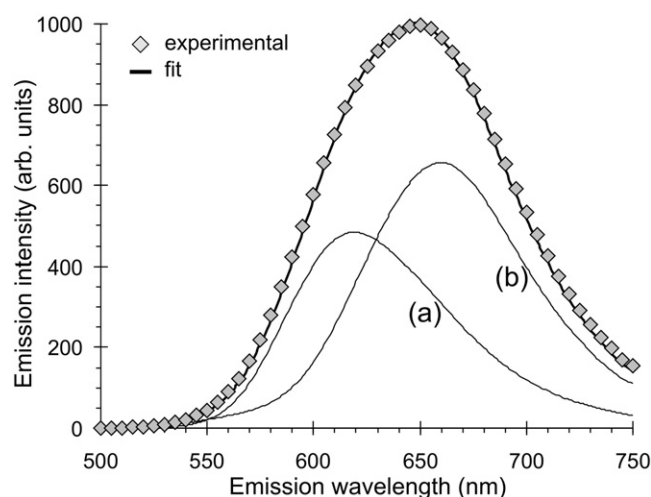


**Figure 7.** PL emission spectra for (a)  $\text{Ca}_{1.2}\text{Eu}_{0.8}\text{SiS}_4$ , (b)  $\text{Ca}_{1.8}\text{Eu}_{0.2}\text{SiS}_4$ . The thick line (fit) is the sum of spectra (a) and (b). ‘Experimental’ is the PL emission spectrum of the powder with an intended composition of  $\text{Ca}_{1.5}\text{Eu}_{0.5}\text{SiS}_4$ .

average 415 pm. Replacing the Eu ions with slightly smaller Ca ions correspondingly reduces the intrachain distance, while in the *ab*-planes the  $\text{SiS}_4$ -tetrahedra remain largely unaffected due to the covalent bonding character. From the Rietveld refinement it was also derived that Ca preferentially substitutes for Eu on the Eu2 site in  $\text{Eu}_2\text{SiS}_4$ . This can be related to the slightly shorter Eu–S distances for the Eu2 site compared to the Eu1 site in  $\text{Eu}_2\text{SiS}_4$ . As a consequence of this preferential substitution, the cation chains along the *c*-axis will be more or less alternately occupied by Ca and Eu ions, which basically leads to a lowering of the symmetry and to the appearance of additional peaks in the diffraction pattern.

Regarding the fully substituted  $\text{Eu}_2\text{SiS}_4$ , its luminescence behaviour is rather similar to that of  $\text{EuGa}_2\text{S}_4$ , which also shows a considerable thermal quenching at room temperature [25]. The presence of non-radiative decay paths strongly reduces the lifetime at room temperature, again similar to  $\text{Eu}_2\text{SiS}_4$ .  $\text{EuGa}_2\text{S}_4$  has been studied as a host for rare-earth doping (for instance with  $\text{Er}^{3+}$ ), as good energetic coupling can then be achieved between the rare-earth ions [25].

An important observation that remains to be discussed is the presence of two emission bands in relatively low Eu-doped  $\text{Ca}_2\text{SiS}_4$  powders. Resuming the experimental results, a yellow emission band (peaking at 564 nm) dominates at low Eu concentration, while a second (red) emission band peaking at 660 nm arises at higher concentration.

As, without any doubt, only one crystalline phase is observed for an Eu concentration of up to 10%, the occurrence of the red emission band in lightly doped powders (figure 2(a)) cannot be explained by the formation of a second phase. Furthermore, the hypothesis by Avella of it being related to the presence of  $\text{CaS:Eu}$  can be rejected in our powders for the following reasons: (i) the relatively strong concentration quenching in  $\text{CaS:Eu}$  powders [26] is in contrast with the red emission in  $\text{Ca}_2\text{SiS}_4\text{:Eu}$ , which is most efficient for about 5% Eu (figure 2(b)); (ii) when no  $\text{CaS}$  peaks are seen in x-ray diffraction patterns, only a marginal amount can be present in the powder, which cannot account for the high quantum efficiency of the red emission in  $\text{Ca}_2\text{SiS}_4\text{:Eu}$  powder; (iii) at 20 K, the red emission peaks at 669 nm (not shown), which is clearly different from  $\text{CaS:Eu}$  at that temperature (656 nm, [27]). Furthermore, no phonon emission peaks are observed in the  $\text{Ca}_2\text{SiS}_4\text{:Eu}$  powder with low dopant concentration at low temperature, in contrast to the prominent phonon lines in  $\text{CaS:Eu}$  [27].

An alternative explanation can be provided by the arrangement of the Ca ions (and consequently the Eu ions upon substitution) in the  $\text{Ca}_2\text{SiS}_4$  unit cell. Based on the data for the isomorphous  $\text{Ca}_2\text{GeS}_4$  compound, two different sites are present for the Ca ions [28]. Although both sites have similar sixfold sulfur coordination, the Ca ions on wyckoff site 4a form chains along the *b*-axis, in contrast to the Ca ions on the 4c positions. The formation of chains results in the preferential orientation of the Eu 5d orbitals, which is known to lower the emission energy [29]. The presence of two emission bands in europium-doped ternary compounds was also reported in, for instance,  $\text{Ca}_2\text{SiO}_4$ ,  $\text{Sr}_2\text{SiO}_4$  and  $\text{Ba}_2\text{SiO}_4$  [29, 30], which can also show cation chains. However, the presence of these cation chains is not sufficient to lead to a lower emission energy and Poort *et al* raised the following restriction [31]: the reduction in emission energy upon incorporation along a chain does not occur when the interchain distance is similar to the intrachain distance. This restriction does not apply for  $\text{Ca}_2\text{SiS}_4$ , as these distances are 0.62 nm and 0.41 nm, respectively. The higher the dopant concentration, the more Eu ions are in proximity to each other, leading to an increased chance of energy transfer. Hence, the red emission will increase relative to the yellow emission, which is observed experimentally.

## 5. Conclusions and perspectives

The emission properties of the  $(\text{Ca}, \text{Eu})_2\text{SiS}_4$  phosphor system are clearly more complicated than could be expected from the previous accounts in the 1970s. Powders with low dopant concentration show two emission bands (at 564 and at 660 nm), for which the energetic coupling was studied by decay measurements. We argued why the red emission band cannot be explained by trace amounts of CaS:Eu in the synthesis, but it most likely originates from the presence of two different sites in the orthorhombic  $\text{Ca}_2\text{SiS}_4$  lattice. At high dopant concentration (>40%), the  $(\text{Ca}, \text{Eu})_2\text{SiS}_4$  phosphors crystallize in the monoclinic,  $\text{Eu}_2\text{SiS}_4$ -like structure. For these powders, the photoluminescence peak shifts almost linearly from 614 to 577 nm on the  $(\text{Ca}, \text{Eu})$  composition. This shift in emission wavelength is related to an anisotropic change in lattice constants. Even the fully substituted  $\text{Eu}_2\text{SiS}_4$  powder shows photoluminescent emission at room temperature, although non-radiative decay paths reduce the efficiency.

The emission properties of  $(\text{Ca}, \text{Eu})_2\text{SiS}_4$  make it worthwhile investigating this phosphor in colour conversion LEDs, as the requirements are largely met:

- (i) The broad excitation spectrum (partly caused by the efficient energy transfer between both emission centres) gives a good overlap with the emission spectrum of the current high-efficiency pumping LEDs, in combination with a high quantum efficiency. The external quantum efficiency of this phosphor reached about 35% for the composition  $\text{Ca}_2\text{SiS}_4:\text{Eu}$  [2%].
- (ii) Depending on the application, the emission colour can be tuned by variation of the Ca:Eu ratio from yellow to saturated red. Furthermore, the emission is characterized by broad-band emission, which is favourable for good colour rendering. Further tuning of the emission properties is possible by considering similar materials, by (partial) substitution of Ca by Mg, Sr or Ba, Si by Ge, or S by Se [13]. This kind of combinatorial approach quickly leads to optimized phosphor materials [12].
- (iii) The stability of this ternary phosphor material is good, certainly when compared to the hygroscopic thioaluminates. Currently, the binary sulfides, like SrS:Eu, have found their way into pcLED applications. The stability of the  $(\text{Ca}, \text{Eu})_2\text{SiS}_4$  powders is comparable to that of CaS and SrS. As pointed out briefly, the stability also depends on the preparation conditions (affecting overall stoichiometry), which leaves opportunities for improvement.

- (iv) The emission colour is stable as a function of temperature (studied up to 320 K) and of the excitation power.

This study shows that a specific class of phosphors, i.e. the thiosilicates, deserves renewed interest despite earlier reports on the poor efficiency in cathodoluminescence. As a photoluminescent material, it shows interesting emissive properties, making it promising for several types of applications, among which are pcLEDs. Future research can aim both at a further fundamental understanding of the emission processes in  $\text{Ca}_2\text{SiS}_4\text{:Eu}$  and at an improvement of the luminescence properties by altering the synthesis conditions.

## Acknowledgments

PFS and JVH both acknowledge financial support by the Bijzonder Onderzoeksfonds (Universiteit Gent). This research is partly sponsored by the Research Foundation-Flanders (FWO-Vlaanderen).

## References

- [1] Dorenbos P 2003 *J. Lumin.* **104** 239–60
- [2] Benalloul P, Barthou C and Benoit J 1998 *J. Alloys Compounds* **277** 709–15
- [3] Miura N, Kawanishi M, Matsumoto H and Nakano R 1999 *Japan. J. Appl. Phys.* **2** **38** L1291–2
- [4] Smet P F, Van Haecke J E, Van Meirhaeghe R L and Poelman D 2005 *J. Appl. Phys.* **98** 043512
- [5] Poelman D, Doerschel J and Smet P F 2004 *Spectrochim. Acta B* **59** 1775–80
- [6] Kumar V, Singh N, Kumar R and Lochab S P 2006 *J. Phys.: Condens. Matter* **18** 5029–36
- [7] Barthou C, Jabbarov R B, Benalloul P, Chartier C, Musayeva N N, Tagiev B G and Tagiev O B 2006 *J. Electrochem. Soc.* **153** G253–8
- [8] Do Y R, Ko K Y, Na S H and Huh Y D 2006 *J. Electrochem. Soc.* **153** H142–6
- [9] Mueller-Mach R, Mueller G, Krames M R, Hoppe H A, Stadler F, Schnick W, Juestel T and Schmidt P 2005 *Phys. Status Solidi a* **202** 1727–32
- [10] Xie R J, Hirotsuki N, Mitomo M, Takahashi K and Sakuma K 2006 *Appl. Phys. Lett.* **88** 101104
- [11] Kim K N, Park J K, Choi K J, Kim J M and Kim C H 2006 *Electrochem. Solid State Lett.* **9** G262–4
- [12] Nazarov M and Yoon C 2006 *J. Solid State Chem.* **179** 2529–33
- [13] Olivierfourcade J, Ribes M, Philippot E, Merle P and Maurin M 1975 *Mater. Res. Bull.* **10** 975–82
- [14] Avella F J 1971 *J. Electrochem. Soc.* **118** 1862–3
- [15] Rocktäschel G, Ritter W and Weiss A 1964 *Z. Naturf. b* **19** 958
- [16] Hartenbach I and Schleid T 2002 *Z. Anorg. Allg. Chem.* **628** 1327–31
- [17] Samura Y, Usui S, Ohmi K and Kobayashi H 2004 *Proc. 12th Int. Workshop on Inorganic and Organic Electroluminescence and 2004 Int. Conf. on the Science and Technology of Emissive Displays and Lighting (Toronto, 2004)*
- [18] Lethi K T, Garcia A, Guillen F and Fouassier C 1992 *Mater. Sci. Eng. B* **14** 393–397
- [19] Roisnel T and Rodriguez-Carvajal J 2001 *Epdic 7: European Powder Diffraction, Pts 1 and 2* vol 378-3, pp 118–23
- [20] Toby B H 2006 *Powder Diffr.* **21** 67–70
- [21] Shionoya S and Yen W M 1999 *Phosphor Handbook* (Boca Raton, FL: CRC Press)
- [22] Johrendt D and Pocha R 2001 *Acta Crystallogr. E* **57** i57–9
- [23] Van Haecke J E, Smet P F and Poelman D 2004 *Spectrochim. Acta B* **59** 1759–64
- [24] Van Haecke J E, Smet P F and Poelman D 2007 *J. Lumin.* **126** 508–14
- [25] Barthou C, Benalloul P, Tagiev B B, Tagiev O G, Abushov S, Kazimova F A and Georgobiani A N 2004 *J. Phys.: Condens. Matter* **16** 8075–84
- [26] Van Haecke J E, Smet P F and Poelman D 2005 *J. Electrochem. Soc.* **152** H225–8
- [27] Yamashita N, Harada O and Nakamura K 1995 *Japan. J. Appl. Phys.* **1** **34** 5539–45
- [28] Ribes M, Philippot E and Maurin M 1970 *C. R. Acad. Sci. Paris C* **270** 716–8
- [29] Poort S H M, Janssen W and Blasse G 1997 *J. Alloys Compounds* **260** 93–7
- [30] Kim J S, Jeon P E, Choi J C and Park H L 2005 *Solid State Commun.* **133** 187–90
- [31] Poort S H M, Reijnhoudt H M, vanderKuip H O T and Blasse G 1996 *J. Alloys Compounds* **241** 75–81